Journal of Ceramic Processing Research. Vol. 4, No. 4, pp. 185~190 (2003)

J O U R N A L O F
Ceramic
Processing Research

Advanced high density plasma processing in inductively coupled plasma systems for plasma-enhanced chemical vapor deposition and dry etching of electronic materials

Jewon Lee*, Wantae Lim, Inkyoo Baek and Guan Sik Cho

School of Nano Engineering/Institute of Nano-Technology Applications, Inje University, Gimhae, Kyoung-Nam 621-749, Korea (ROK)

Plasma processing is one of the key steps for the fabrication of many advanced electronic and photonic devices, such as DRAM, heterojunction bipolar transistors, lasers, LEDs, micro-magnetic drives, and planar lightwave circuits. High density plasma technologies are becoming popular for pattern transfer and chemical vapor deposition (CVD) of electronic and dielectric materials. Inductively coupled plasma (ICP) etching results have shown that it is possible to achieve excellent process recipes for compound semiconductors. ICP-PECVD also provided great advantages for low-temperature (<150°C) SiNx deposition technology. These data encouraged an expansion of the application of high density plasma processing for manufacturing of new opto-electronic devices. This paper will report recent developments of SiNx deposition and GaAs etching results in inductively coupled plasma systems.

Key words: Plasma Processing, PECVD, Dry etching, SiNx, GaAs, inductively coupled plasma.

Introduction

There is a growing interest in high-density plasma processing in both the semiconductor and the magnetic thin film head industry [1-7]. In particular, much research has been conducted on dry etching with inductively coupled plasma (ICP) sources because they provide advanced processes for pattern transfer [8-10]. A great deal of research has been reported for dielectric film deposition using remote or high-density plasmas. [11-14] However, there has been relatively little work on deposition technology for dielectric materials using ICP [15, 16]. Using an ICP source, we have explored high-density plasma ($>10^{11}$ cm^{-3}) chemical vapor deposition (HDPCVD) of SiN_x and SiO_2. In comparing HDPCVD technology with conventional PECVD, some potential advantages are lower hydrogen content films, higher quality films at lower process temperatures (<200°C), void-free gap filling of high aspect ratio features, and self-planarization. Low temperature SiN_x film deposition of low hydrogen content by HDPCVD is of special interest for cap and capacitor layers in III-V semiconductor devices [17-21]. Due to the relatively low dissociation efficiency of N_2, typical process recipes for SiN_x deposition by PECVD use NH_3 as the source of nitrogen. Therefore, some portion of hydrogen incorporation from NH_3 in deposited SiN_x films is inevitable. However, HDPCVD technology enables us to deposit SiN_x with a NH_3-free recipe because high-density plasma sources have typically one order of magnitude higher ion dissociation efficiency (i.e. ~0.1 % for PECVD and ~1% for HDPCVD).

Some advantages of an ICP source over other types of high-density sources include easier scale up, advanced automatic tuning for the source, and lower cost of ownership. In addition, with a hybrid ICP configuration, such as was used in this work, it is possible through the addition of RF power to the wafer chuck, to control the ion flux and ion energy independently. This expands the applications for dielectric film deposition by ICP. For example, gap-filling techniques require simultaneous high ion bombardment by an inert gas, such as Ar, during deposition to prevent void formation. To achieve high ion bombardment, high ion energy can be induced by controlling the RF power on the wafer chuck in HDPCVD without a change to the ion density in the source. In PECVD, this approach is not feasible and alternating sequences of deposition and sputter etch are usually required. This requires extra steps and more process time. For damage-sensitive devices, such as the high electron mobility transistor (HEMT), it is essential to use a very low ion energy process because ion energy is a major factor causing ion damage to the device [22]. With HDPCVD, the ion energy can be reduced to minimize damage of the devices. The process pressures for PECVD and HDPCVD are quite different. More than 500 mTorr is common for PECVD. The pressure range of HDPCVD is 1 to 30 mTorr. We

*Corresponding author:
Tel : 82-55-320-3718
Fax: 82-55-320-3631
E-mail: jwlee@inje.ac.kr

will report on the effect of RF chuck power and pressure for SiN_x films deposited by HDPCVD with an ICP source.

A planar ICP system that we recently developed had very interesting properties. It ignited and held a very low power ICP plasma (even as low as 100 W). Additionally, the ICP plasma easily ignited and maintained itself with a pure ICP source power alone. No RIE chuck power was applied for the ignition. This may provide a new regime of plasma processing for materials with minimum damage and very precise control of etch rate. We will also discuss the etching results of GaAs in a BCl_3 planar inductively coupled plasma in this paper.

Experimental

Both SiN_x and SiO_2 films were deposited in a Unaxis' ICP-CVD system on 4 (100 mm) Si wafers. Figure 1 shows a schematic of the ICP chamber configuration. The load module of the system can handle up to about 50 wafers at a time. For the SiN_x deposition, two different gas chemistries, $SiH_4/N_2/Ar$ and $SiH_4/NH_3/He$, were explored. A gas chemistry of $SiH_4/O_2/Ar$ was used for the SiO_2 film deposition. Electronic mass flow controllers regulated all gas flows. The SiH_4 was fed through a lower gas ring (gas inlet 2). All other gases entered the chamber via a showerhead in the ICP source (gas inlet 1). The process chamber is a hybrid configuration consisting of an inductively coupled plasma (ICP) source and an RF powered wafer chuck. An oil recirculating heat exchanger connected to the chuck controls the wafer temperature. Helium backside cooling of the wafer is used for efficient heat transfer. For this work, the ICP source power and chuck temperature were fixed at 800 W and 150°C respectively. We have found that lower deposition temperatures lead to poor quality dielectrics with relatively high wet etch rates. The RF chuck power and chamber pressure were varied from 25 to 150 W and 1 to 20 mTorr, respectively.

The deposition rate and uniformity were determined by a NanoSpec model 4150 metrology system. Refractive index measurements were made on a Gaertner model L116D-PC ellipsometer. Film stress measurements were done with a Tencor model P-2 profilometer. A buffered oxide etch (BOE) solution of 7:1 NH_4:HF was used for the wet-etch rate measurements.

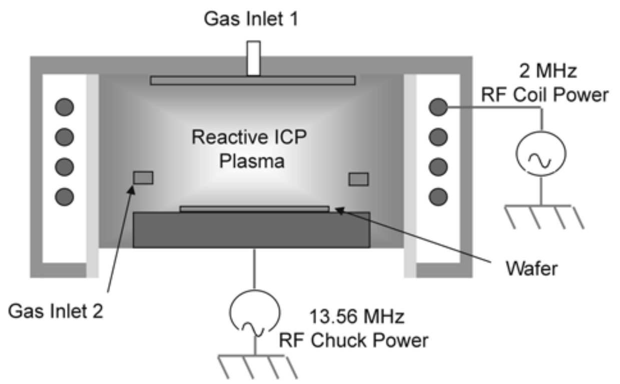

Fig. 1. Schematic of the ICP chamber.

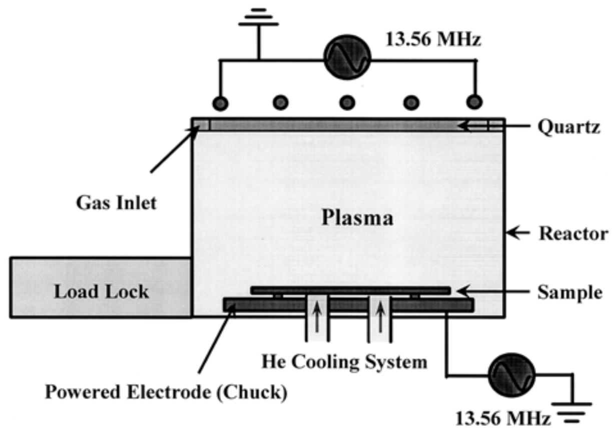

Fig. 2. Schematic of a planar inductively coupled plasma etching reactor.

We used a planar ICP system for GaAs dry etching. The system (Model No. APE510) was manufactured by Cliotek, Inc. The system had a mechanical pump and a turbo molecular pump for low pressure processing. A simple schematic of the planar ICP system is shown in Figure 2. Both of the RIE chuck power (maximum 500 W) and ICP source power (maximum 1000 W) used 13.56 MHz-based RF power generators and matching networks. The system could handle a 4 inch (100 mm) size wafer with a clamp. A patterned GaAs wafer with a photo resist was cut into small pieces (1×1 cm^2) for each run. The thickness of photo resist was 1 µm. Some bare GaAs samples were also inserted in to the system for surface study after plasma exposure. All samples were mounted on a 4 inch (100 mm) round anodized aluminum carrier with a vacuum heat sink paste before each run. The ICP source power was varied from 0 to 500 W during experiment. The RIE chuck power was changed from 0 to 150 W. Chamber pressure and BCl_3 gas flow were controlled from 5 to 15 mTorr and 10 to 40 standard cubic centimetre per minute (sccm). Etch time was varied from 3 to 5 minutes in order to have a reasonable etch depth of the GaAs. The etch depth was measured by surface stylus profilometry (Alpha step -200) after photo resist (PR) removal with acetone. Surface morphology and sidewall passivation was characterized by Scanning Electron Microscopy (SEM). Surface roughness was measured by an Atomic Force Microscope (AFM). Surface residues after etching were characterized with a ESCALAB 250 XPS spectrometer in KBSI Busan Branch.

Results and Discussion

Silicon Nitride Deposition in $SiH_4/N_2/Ar$ ICP processing

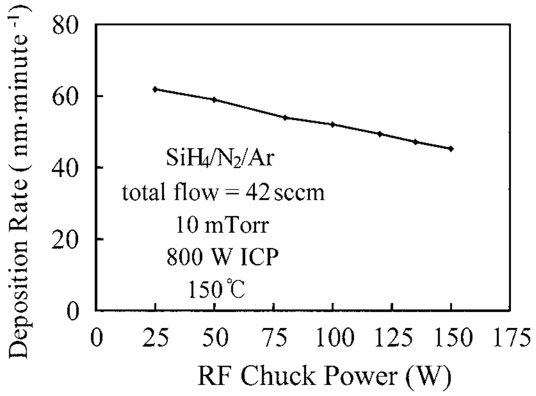

Fig. 3. SiN_x deposition rate as a function of RF chuck power.

Figure 3 shows the dependence of deposition rate on RF chuck power for SiNx deposition with $SiH_4/N_2/Ar$ ICP processing. The deposition rate decreases with increasing RF chuck power. At high RF power, it is expected that more ion bombardment during deposition will occur. High RF power increases the dc bias and consequently the ion energies of the bombarding species, e.g. Ar^+ and N_2^+, will increase. This will enhance the sputtering of Si and N reactive neutrals before and during the formation of the SiN_x film. This accounts for the observed reduction in deposition rate with RF power. The typical deposition rate was in the range 40 to 60 nm·minute^{-1}. This is comparable to conventional PECVD using the same precursors at much higher pressures.

Figures 4 and 5 show the variation of refractive index and BOE rate with RF chuck power. At 25 W RF chuck power, a refractive index of 1.95 was achieved. The combination of decrease of deposition rate and BOE rate, and increase of refractive index with RF chuck power indicates that the deposited films become slightly Si-rich (Si fraction increased from 0.51 to 0.57). This was confirmed by Auger Electron Spectroscopy (AES) measurements.

One possible explanation for the increase of refractive index with RF power is that the dissociation of SiH_4 into reactive neutrals in the $SiH_4/N_2/Ar$ plasma increased relative to that of N_2 with RF chuck power (in other words, ion energy). Another possible explanation is that high RF power brings more Si-related species than N to participate in the film growth. Table 1 shows the dissociation energy of related diatomic molecules for SiN_x deposition. Notice that the N-N bond has a much higher bond strength (945.33 kJ/mol) than that of Si-H (≤299.2 kJ/mol). Dissociation of N_2 requires more energy than that of SiH_4. All of these data suggests that more SiH_4 species are brought to the substrate than N_2 with increase of RF chuck power.

It is worthwhile commenting further on the BOE data presented in Figure 5. Considering the low deposition temperature of 150°C, the typical BOE rate of 100 nm·minute^{-1} is very low. At 150°C, the BOE rate of PECVD SiN_x is greater than 500 nm·minute^{-1}. This implies that the ICPCVD SiN_x films are denser and

Table 1. Dissociation energies of diatomic molecules

Bond	Dissociation Energy at RT (kJ/mol)
Si-H	≤ 299.2
N-H	≤ 339
N-N	945.33
H-H	435.99

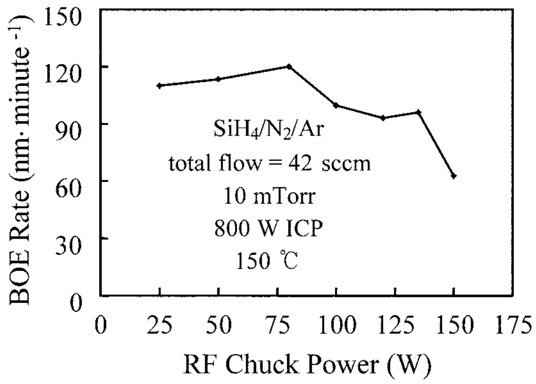

Fig. 5. BOE rate of ICPCVD SiN_x as a function of RF chuck power.

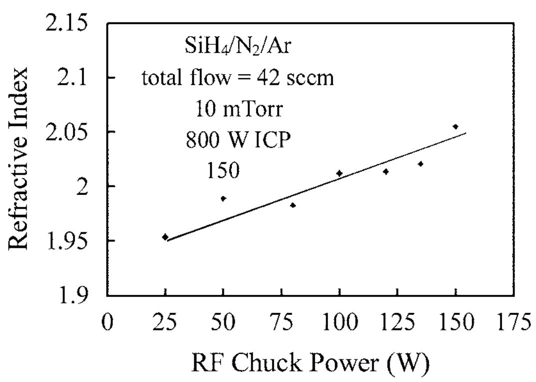

Fig. 4. Refractive index of ICPCVD SiN_x as a function of RF chuck power.

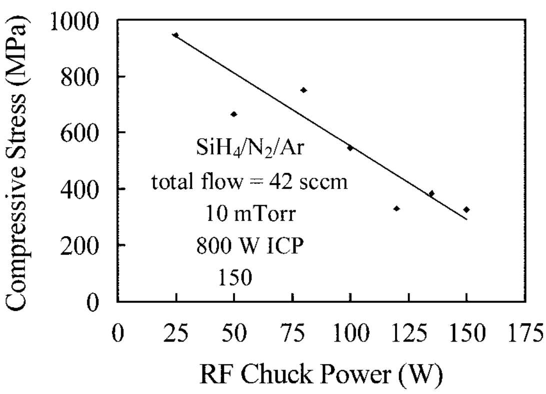

Fig. 6. Compressive stress of ICPCVD SiN_x as a function of RF chuck power.

contain less hydrogen [25].

As indicated in Figure 6, the stress of all ICPCVD SiN_x films prepared from $SiH_4/N_2/Ar$ was compressive. At 25 W RF chuck power, the film stress was as high as 900 MPa. Raising the RF chuck power lowers the film stress. A stress of 300 MPa is achieved at 120 W. A film stress of less than 500 MPa is acceptable for many applications. We speculate that incorporated hydrogen relieves the stress in the SiN_x film, although the correlation with RF chuck power is not fully understood. The typical H content in our SiNx films ranged from 15-20 at.%. compared to 25-30 at.% for PECVD films deposited at the same temperatures. In PECVD, the film stress increases with RF power regardless of whether it is compressive or tensile. This is drametrically opposite to the current observations with ICP-CVD.

Inductively Coupled Plasma Etching of GaAs

Figure 7 shows GaAs etch rates, etch selectivity to a photo resist (PR) and negatively induced dc bias as a function of ICP source power after dry etching in the planar ICP system. The GaAs etch rate almost linearly increased with ICP source power. The etch selectivity of GaAs to a PR also increased with ICP source power. Notice that the etch rate increased from 180 nm·minute^{-1} to 620 nm·minute^{-1} when the ICP source power was changed from 0 to 500 W at 20 BCl_3, 100 W RIE chuck power and 7.5 mTorr chamber pressure. Selectivity also increased from 2.5:1 to 6:1 when the ICP source increased from 0 W to 500 W a the fixed condition. Therefore, an increase of ICP source power was quite beneficial for high rate and high selectivity GaAs etching during ICP BCl_3 etching. Note also that it was possible to achieve low ICP power (100 W) etching of GaAs at a planar ICP reactor, which would be a great challenge in a cylindrical ICP system. Meanwhile, the decrease of -dc bias was not significant with the increase of ICP source power up to 500 W. The dc bias decreased from -400 V to -320 V when the ICP source power increased from 0 to 500 W.

Figure 8 shows the etch rate of GaAs and etch selectivity to a PR as a function of RIE chuck power. Notice that we could have 280 nm·minute^{-1} of GaAs etch rate with selectivity of 6.5:1 to a PR even only with pure ICP source power at 0 W RIE chuck power. An etch rate of 280 nm·minute^{-1} was still a relatively high etch rate and selectivity of 6.5:1 was an excellent result. This showed that pure ICP power etching could be a very interesting process technique for engineering purposes for low-damage high rate dry etching of GaAs since we could achieve high rate etching with a simple ICP source power without the assistance of RIE chuck power. Note that the selectivity decreased from 6.5:1 to 3.5:1 when the RIE chuck power increased from 0 W to 150 W while the etch rate of GaAs continuously increased from 280 nm·minute^{-1} to 400 nm·minute^{-1} with the same RIE power change. This showed that an increase of dc bias degraded the selectivity of GaAs to a photo resist with energetic ion-bombardment on photo resist at high RIE chuck power. The -dc bias voltage increased with RIE chuck power. It reached -520 V with 150 W RIE chuck power at 20 BCl_3, 300 W ICP and 7.5 mTorr chamber pressure. Both Figure 8 and 9 show that the planar ICP system could be a very efficient tool for excellent independent power control at even very low ICP source power for advanced plasma processing, which has been a great

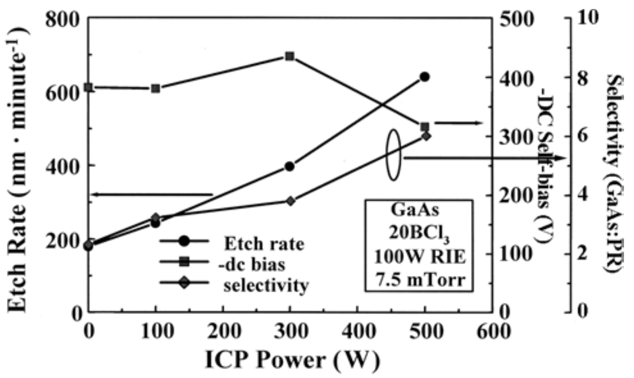

Fig. 7. GaAs etch rate and selectivity to PR, and dc bias as a function of ICP source power (W).

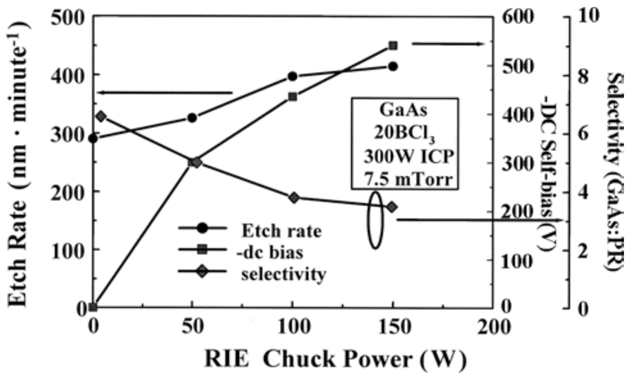

Fig. 8. GaAs etch rate and selectivity to PR, and dc bias as a function of RIE chuck power.

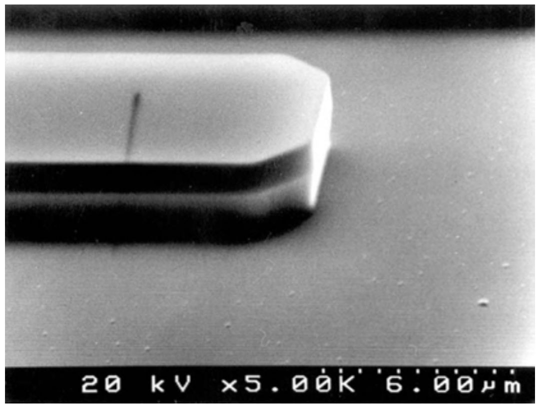

Fig. 9. Scanning Electron Microscopy photos of etched GaAs. PR was still in the place.

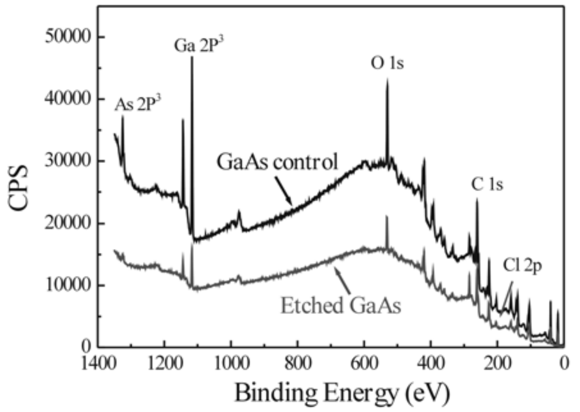

Fig. 10. X-ray Photoelectron Spectroscopy data of etched GaAs surface at 20 BCl_3, 300 W ICP, 100 W RIE and 7.5 mTorr.

challenge for other types of high density ICP plasma systems.

Scanning Electron Microscope (SEM) photo of an etched GaAs feature is shown in Figure 9. The photo resist was still in place. The etch conditions were 20 BCl_3, 300 W ICP source power, 100 W RIE chuck power, 7.5 mTorr. Notice that we obtained an extremely clean and quite vertical sidewall of features after etching. The etch depth of GaAs was 1.2 µm with 0.6 µm thick PR left. The photo resist was easily removed with acetone after etching with these conditions.

Surface residues after planar ICP BCl_3 etching of GaAs were investigated with X-ray photoelectron spectroscopy (XPS). Figure 10 shows XPS data for a GaAs control and a GaAs etched at 20 BCl_3, 300 W ICP, 100 W RIE and 7.5 mT. Again, the etch depth of the GaAs was 1.2 µm. The XPS data showed that there was no distinct peak of BCl_3-related residues on the surface of etched GaAs.

Summary and Conclusions

We investigated low temperature deposition (150°C) of ICP-CVD SiN_x prepared from $SiH_4/N_2/Ar$. For SiN_x films, RF chuck power increased the refractive index while it decreased the deposition rate, stress, and BOE rate. Increasing the RF chuck power may bring more Si species than N species to the wafer surface leading to Si-rich films. The BOE rate of ICPCVD SiN_x, prepared from $SiH_4/N_2/Ar$ is much lower compared to PECVD SiN_x deposited at the same low temperature. This implies that the ICPCVD SiN_x films are denser and contain less hydrogen.

We also investigated GaAs etching in a planar ICP system. It is noted that it was possible to have high rate dry etching of GaAs at low ICP power without RIE power, which would be helpful for etching damage-sensitive compound semiconductors. The dry etching results of GaAs at the moderate conditions in the planar ICP system showed very good sidewall passivation, clean surfaces, smooth morphology, a high GaAs etch rate and high selectivity to PR. An increase of ICP power and RIE chuck power strongly raised GaAs etch rate. In conclusion, inductively coupled plasma technology has many potential advantages compared to typical plasma enhanced chemical vapor deposition and reactive ion etching in a broad range of advanced processes for electronic device fabrication.

Acknowledgments

This work was supported by grant No. (R05-2002-000-01368-0) from the Basic Research Program of the Korea Science & Engineering Foundation. The authors appreciate technical assistance from colleagues at Unaxis, Inc. and Cliotek, Inc.

References

1. C. Constantine, C. Barratt, S.J. Pearton, F. Ren and J.R. Lothian, Appl. Phys. Lett. 61 (1992) 2899-2903.
2. J.W. Lee, H. Cho, C. Hays, C.R. Abernathy, S.J. Pearton, R.J. Shul and G.A. Vawter and H. Han, IEEE J. of Selected Topics in Quantum Electronics 4 (1998) 557-562.
3. F. Ren, J.W. Lee, C.R. Abernathy, S.J. Pearton, C. Constantine, C. Barratt and R. J. Shul, J. Vac. Sci. Technol. B 15 (1997) 983-988.
4. S.J. Pearton, J.W. Lee, E.S. Lambers, J.R. Mileham, C.R. Abernathy, W.S. Hobson and F. Ren, J. Vac. Sci. Technol. B 14 (1996) 118-121.
5. S. Thomas III, K.K. Ko and S.W. Pang, J. Vac. Sci. Technol. A 13 (1994) 894-899.
6. K.B. Jung, J. Hong, H. Cho, S. Onishi, D. Johnson, Y.D. Park, J.R. Childress and S.J. Pearton, J. Vac. Sci. Technol. A 17 (1999) 535-539.
7. R.J. Shul, G.B. McClellan, R.D. Briggs, D.J. Rieger, S.J. Pearton, C.R. Abernathy, J.W. Lee, C. Constantine and C. Barratt, J. Vac. Sci. Technol. A 15 (1997) 633-637.
8. J.W. Lee, E.S. Lambers, C.R. Abernathy, S.J. Pearton, R.J. Shul, F. Ren, W.S. Hobson and C. Constantine, Solid-State Electron. 42 (1998) A65-A73.
9. R.J. Shul, C.G. Wilson, M.M. Bridges, J. Han, J.W. Lee, S.J. Pearton, C.R. Abernathy, J.D. MacKenzie, L. Zhang and L.F. Lester, J. Vac. Sci. Technol. A 16 (1998) 1621-1625.
10. F. Ren, J.W. Lee, C.R. Abernathy, R.J. Shul, C. Constantine and C. Barratt, Semicond. Sci. Tech. 12 (1997) 1154-1160.
11. G. Lucovsky, P.D. Richard, D.V. Tsu, S.Y. Lin and R.J. Markunas, J. Vac. Sci. Technol. A 4 (1986) 681-685.
12. C.B. Labelle, S.J. Limb and K.K. Gleason, J. Appl. Phys. 82 (1997) 1784-1789.
13. S.J. Limb, C.B. Labelle, K.K. Gleason, D.J. Edell and E.F. Gleason Appl. Phys. Lett. 68 (1996) 2810-2816.
14. M. Lapeyrade, M.P. Besland, C. Mevaa, A. Sibai and G. Hollinger, J. Vac. Sci. Technol. A 17 (1999) 433-437.
15. Y.B. Hahn, J.W. Lee, K.D. Mackenzie, D. Johnson, S.J. Pearton and F. Ren, Solid-State Electron. 42 (1998) 2017-2022.
16. Y.B. Hahn, J.W. Lee, K.D. Mackenzie, D. Johnson, D. Hays, C.R. Abernathy and S.J. Pearton, Electrochemical and Solid-State Lett. 1 (1998) 230-235.
17. J.W. Lee, K.D. Mackenzie, D. Johnson, R.J. Shul, S.J. Pearton, C.R. Abernathy and F. Ren, Solid-State Electron.

42 (1998) 1031-1037.
18. J.W. Lee, C.R. Abernathy, S.J. Pearton, F. Ren, R.J. Shul, C. Constantine and C. Barratt, Solid-State Electron. 41 (1997) 829-835.
19. F. Ren, J.W. Lee, C.R. Abernathy, S.J. Pearton, R.J. Shul, C. Constantine and C. Barratt, Semicond. Sci. Technol. 12 (1997) 1154-1160.
20. A. Kapila and V. Malhota, Electrochem. Soc. Proc. 97-21 (1997) 322-327.
21. R.E. Sah, V. Weiman, H. Baumann, J. Wagner, R. Kiefer and S. Muller, Electrochem. Soc. Proc. 97-1 (1997) 179-187.
22. J.W. Lee, K.D. Mackenzie, D. Johnson, R.J. Shul, S.J. Pearton, C.R. Abernathy and F. Ren, Solid-State Electron. 42 (1998) 1021-1027.